Supporting Information:

Quasi-Ballistic Thermal Transport Across MoS_2 Thin Films

Aditya Sood[1,2,†,‡,*], *Feng Xiong*[3,‡], *Shunda Chen*[4], *Ramez Cheaito*[2], *Feifei Lian*[1,¶], *Mehdi Asheghi*[2], *Yi Cui*[5,6], *Davide Donadio*[4,7], *Kenneth E. Goodson*[2,5], *Eric Pop*[1,5,8,*]

[1]Department of Electrical Engineering, Stanford University, Stanford, CA 94305, USA. [2]Department of Mechanical Engineering, Stanford University, Stanford, CA 94305, USA. [3]Department of Electrical and Computer Engineering, University of Pittsburgh, Pittsburgh, PA 15261, USA. [4]Department of Chemistry, University of California, Davis, CA 95616, USA. [5]Department of Materials Science and Engineering, Stanford University, Stanford, CA 94305, USA. [6]Stanford Institute for Materials and Energy Sciences, SLAC National Accelerator Laboratory, Menlo Park, CA 94025, USA. [7]Ikerbasque, Basque Foundation for Science, E-48011 Bilbao, Spain. [8]Precourt Institute for Energy, Stanford University, Stanford, CA 94305, USA. [†]Present address: Stanford Institute for Materials and Energy Sciences, SLAC National Accelerator Laboratory, Menlo Park, CA 94025, USA. [¶]Present address: NG Next Basic Research Laboratory, Northrop Grumman Corporation, Redondo Beach, CA 90278, USA. [‡]Equal contribution.

[*]Corresponding authors: aditsood@alumni.stanford.edu, epop@stanford.edu

1. TDTR sensitivity analysis

To determine TDTR measurement sensitivity to the different parameters of interest, we calculate the sensitivity coefficients S_α as follows:

$$S_\alpha = \frac{\partial \log(Signal)}{\partial \log(\alpha)}$$

where *signal* could either refer to the normalized *in-phase voltage* (V_{in}) or the *ratio* (= - V_{in}/V_{out}), and the parameter α could be the cross-plane thermal conductivity κ_z, the Al/MoS_2 thermal boundary conductance (TBC) G_1, or the MoS_2/SiO_2 TBC G_2. These are plotted in Figure S1 for a 20 nm thick film (a, b), and a 200 nm thick film (c, d).

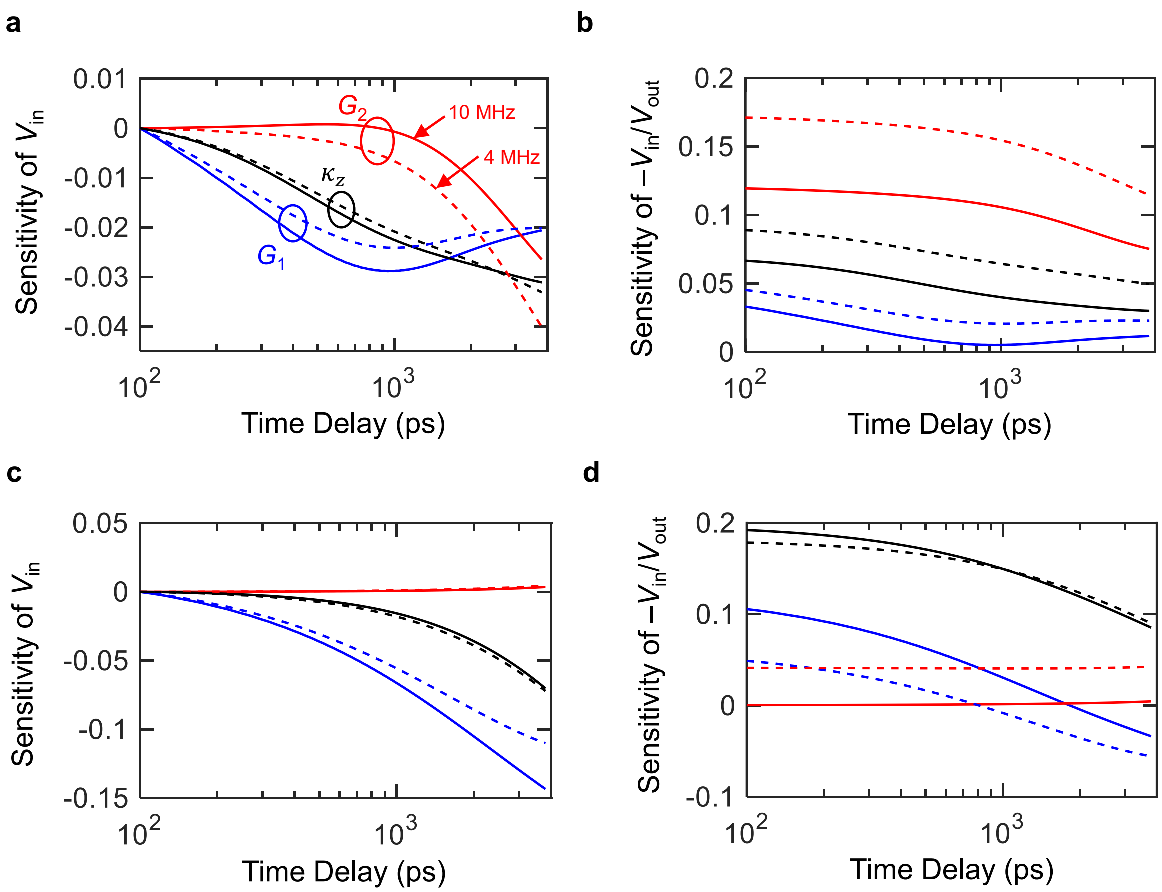

Figure S1. Sensitivity coefficients plotted for (a),(b): t = 20 nm, G_1 = 70 $MWm^{-2}K^{-1}$, G_2 = 25 $MWm^{-2}K^{-1}$, κ_z = 0.9 $Wm^{-1}K^{-1}$, and (c),(d): t = 200 nm, G_1 = 34 $MWm^{-2}K^{-1}$, G_2 = 21 $MWm^{-2}K^{-1}$, κ_z = 2 $Wm^{-1}K^{-1}$. Legend: black (κ_z), blue (G_1), red (G_2). Solid lines (10 MHz), dashed lines (4 MHz).

2. Thermal boundary conductance (TBC) measurements

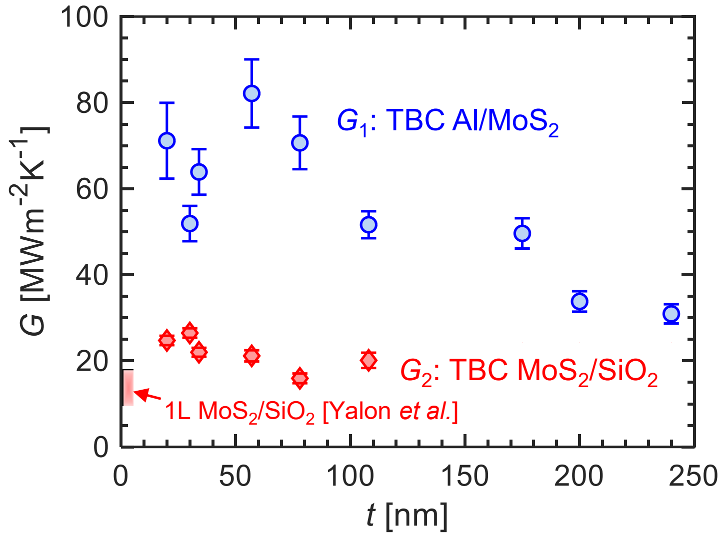

Figure S2. Al/MoS_2 (G_1) and MoS_2/SiO_2 (G_2) TBCs plotted versus film thickness t, shown by the blue circles and red diamonds, respectively. Also shown for comparison are TBC measurements between monolayer MoS_2 and SiO_2 obtained by Raman thermometry[1,2] (red shaded region represents the error bars of the reported result).

3. Thermal penetration depth calculations

To calculate the thermal penetration depth (d_p) in the TDTR measurements, we solve the full 3D heat diffusion equation in the multilayer stack. This is solved in the frequency domain under a sinusoidal heat flux excitation using methods described elsewhere[3,4]. We compute the amplitude of temperature oscillations $\Delta T(r,z)$ at the modulation frequency f_mod; d_p is the distance from the top surface at which $\Delta T(r,z)$ is reduced to $1/e$ of its maximum value.

Figure S3(a) shows $\Delta T(r,z)$ within a 300 nm thick MoS_2 film – this case is representative of one of the thick samples measured in our study (for which $\kappa_\mathrm{z} \sim 2$ $Wm^{-1}K^{-1}$). The simulation is carried out on a multilayer stack of Al/MoS_2/SiO_2/Si using a 4-layer model. The thermal properties of the various layers are provided in the main text. The TBCs of the Al/MoS_2 and MoS_2/SiO_2 interfaces are 40 $MWm^{-2}K^{-1}$ and 20 $MWm^{-2}K^{-1}$ respectively, although these do not affect d_p significantly. The heat flux is modulated at f_mod = 4 MHz, since this is the frequency at which we extract κ_z. Note that d_p is affected both by f_mod and the laser spot diameter (w_0); in these simulations, w_0 = 3 µm. Figure S3(b) plots $\Delta T(z)$ at r = 0. From this we estimate $d_\mathrm{p} \approx$ 160 nm.

The same procedure is used to calculate d_p for the bulk samples measured in previous studies[5–7] using a 2-layer model (Al/MoS_2). In each case, the simulations are performed using the reported κ_z, f_mod and w_0 values. A representative calculation[5] is shown in Figures S3(c),(d).

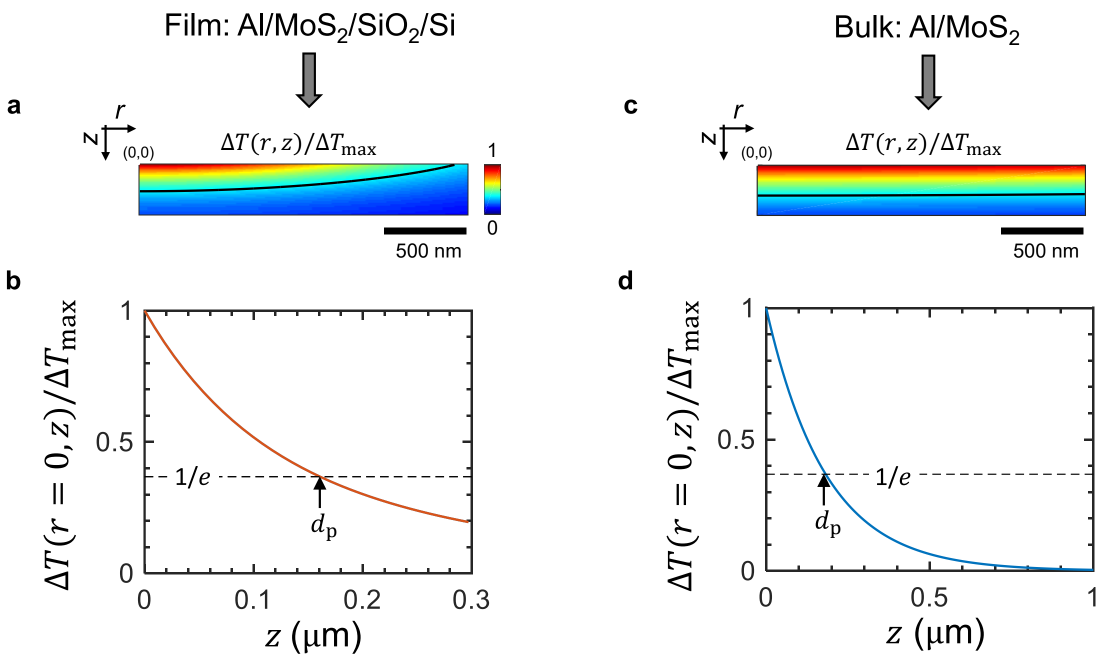

Figure S3. (a) Normalized amplitude of temperature oscillations in a 300 nm thick MoS_2 film with $\kappa_z = 2$ $Wm^{-1}K^{-1}$, $f_{\mathrm{mod}} = 4$ MHz, $w_0 = 3$ µm. The film is part of a multilayer stack: $Al/MoS_2/SiO_2/Si$, representative of the samples measured in this study. (b) Line-out along $r = 0$, with the dashed line indicating a $1/e$ thermal penetration depth of $d_{\mathrm{p}} \approx 160$ nm. (c) Normalized amplitude of temperature oscillations in a bulk MoS_2 substrate[5] with $\kappa_z = 2$ $Wm^{-1}K^{-1}$, $f_{\mathrm{mod}} = 9.8$ MHz, $w_0 = 24$ µm. (d) Line-out along $r = 0$, indicating $d_{\mathrm{p}} \approx 180$ nm.

4. Phonon wavelength contributions to thermal conductivity

We use DFT calculations to determine the range of phonon wavelengths that contribute to thermal transport along the c-axis. Figure S4 shows the thermal conductivity accumulation function plotted versus wavelength at 300 K. Based on this, the median wavelength is $\lambda \sim 1.5$ nm. If we posit that the MoS_2 film must have a thickness of at least $\sim 3\lambda$ in order to have a '3D' phonon dispersion, we estimate a minimum thickness of ~5 nm. For $t < 5$ nm, more detailed calculations may be needed to understand the effect of confinement on phonon band structure and cross-plane thermal transport.

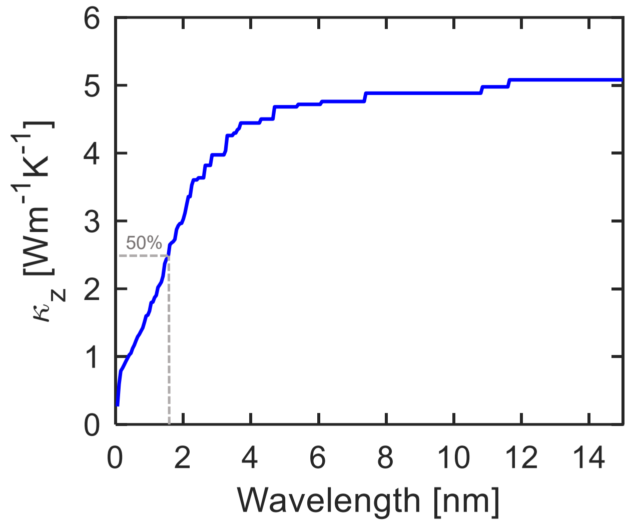

Figure S4. Calculated cumulative distribution function of the cross-plane thermal conductivity (κ_z) versus phonon wavelength at 300 K.

5. Cross-plane thermal transport in thin-film graphite and few-layer graphene

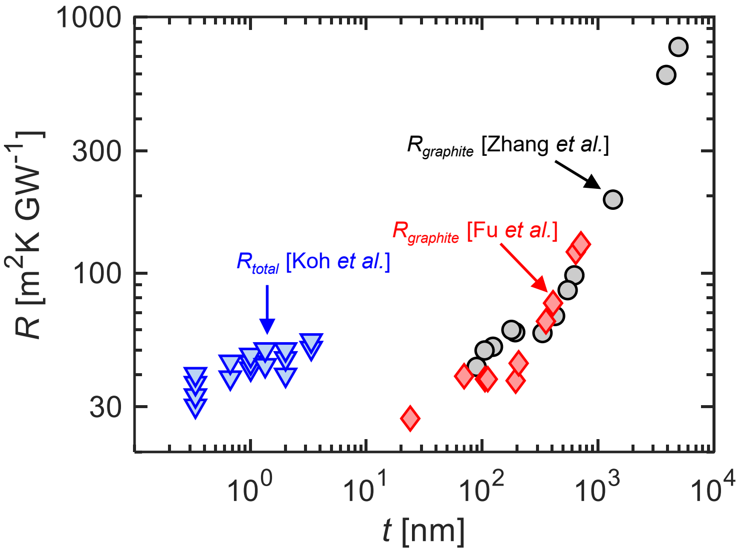

Figure S5. A summary of cross-plane thermal resistance measurements of crystalline graphite thin-films and few-layer graphene from literature. Intrinsic cross-plane thermal resistance measurements are from Zhang *et al.*[8] (90 nm < t < 5 µm), shown in black circles, and Fu *et al.*[9] (24 nm < t < 714 nm), shown in red diamonds. The intrinsic resistance is defined as $R_{\mathrm{graphite}} = t/\kappa_z$. For the case of Fu *et al.*[9] this is calculated by subtracting out the estimated interface contribution. Total cross-plane thermal resistance measurements of Au/Ti/few-layer-graphene/SiO_2 interfaces for 0.3 < t < 3 nm are from Koh *et al.*[10], shown as blue triangles; the total resistance including the interfacial contribution is $R_{\mathrm{total}} = R_{\mathrm{n-graphene}} + R_{\mathrm{interfaces}}$. The plateau in intrinsic thermal resistance in Zhang *et al.*[8] and Fu *et al.*[9] could be related to the onset of quasi-ballistic thermal transport. A comparison to the total thermal resistance values for few-layer-graphene by Koh *et al.*[10] suggests that a contributing factor to the thickness-independent R_{total} could be the strongly-ballistic transport of thermal phonons propagating along the c-axis of the thin-films.

References

(1) Yalon, E.; Mcclellan, C. J.; Smithe, K. K. H.; Xu, R. L.; Rojo, M. M.; Suryavanshi, S. V.; Gabourie, A. J.; Neumann, C. M.; Xiong, F.; Pop, E. Energy Dissipation in Monolayer MoS_2 Electronics. *Nano Lett.* **2017**, *17* (6), 3429–3433.

(2) Yalon, E.; Aslan, Ö. B.; Smithe, K. K. H.; McClellan, C. J.; Suryavanshi, S. V.; Xiong, F.; Sood, A.; Neumann, C. M.; Xu, X.; Goodson, K. E.; Heinz, T. F.; Pop, E. Temperature-Dependent Thermal Boundary Conductance of Monolayer MoS_2 by Raman Thermometry. *ACS Appl. Mater. Interfaces* **2017**, *9* (49), 43013–43020.

(3) Cahill, D. G. Analysis of Heat Flow in Layered Structures for Time-Domain Thermoreflectance. *Rev. Sci. Instrum.* **2004**, *75* (12), 5119–5122.

(4) Braun, J. L.; Hopkins, P. E. Upper Limit to the Thermal Penetration Depth during Modulated Heating of Multilayer Thin Films with Pulsed and Continuous Wave Lasers: A Numerical Study. *J. Appl. Phys.* **2017**, *121*, 175107.

(5) Liu, J.; Choi, G. M.; Cahill, D. G. Measurement of the Anisotropic Thermal Conductivity of Molybdenum Disulfide by the Time-Resolved Magneto-Optic Kerr Effect. *J. Appl. Phys.* **2014**, *116*, 233107.

(6) Jiang, P.; Qian, X.; Gu, X.; Yang, R. Probing Anisotropic Thermal Conductivity of Transition Metal Dichalcogenides MX_2 (M = Mo, W and X = S, Se) Using Time-Domain Thermoreflectance. *Adv. Mater.* **2017**, *29* (36), 1701068.

(7) Muratore, C.; Varshney, V.; Gengler, J. J.; Hu, J. J.; Bultman, J. E.; Smith, T. M.; Shamberger, P. J.; Qiu, B.; Ruan, X.; Roy, A. K.; Voevodin, A. A. Cross-Plane Thermal Properties of Transition Metal Dichalcogenides. *Appl. Phys. Lett.* **2013**, *102*, 081604.

(8) Zhang, H.; Chen, X.; Jho, Y. D.; Minnich, A. J. Temperature-Dependent Mean Free Path

Spectra of Thermal Phonons along the *c*-Axis of Graphite. *Nano Lett.* **2016**, *16* (3), 1643–1649.

(9) Fu, Q.; Yang, J.; Chen, Y.; Li, D.; Xu, D. Experimental Evidence of Very Long Intrinsic Phonon Mean Free Path along the *c*-Axis of Graphite. *Appl. Phys. Lett.* **2015**, *106*, 031905.

(10) Koh, Y. K.; Bae, M. H.; Cahill, D. G.; Pop, E. Heat Conduction across Monolayer and Few-Layer Graphenes. *Nano Lett.* **2010**, *10* (11), 4363–4368.